Dust mass in simulations of galaxies

Nicolas Gaudin⋆ and Hervé Wozniak⋆

⋆ Observatoire Astronomique de Strasbourg, Université de Strasbourg, CNRS

Introduction

We have introduced calculation of dust abundance in self-consistent chemodynamical N-body+SPH simulations [10,15] of galaxies to investigate the properties of this ISM component.

In particular we focus on the dust vs oxygen mass trend that has been observed for a full range of metallicities. We show that our sophisticated simulations are able to reproduce the observational trend provided that all formation and destruction mechanisms are properly implemented.

The simulated ISM is made of two gaseous phases in pressure equilibrium, the cold phase (CP) with a constant temperature at $T \sim 100$ K that mimics the CNM, and the warm–hot phase (WHP) of varying temperature $T > 100$ K to represent the WNM, WIM and HIM. The cooling function is computed in real time according to the elemental chemical composition. Evaporation and condensation allow phase transitions. The feedback includes secular stellar winds, SNIa and SNII explosions. Star formation occurs in the CP according to recipes based on a local Jeans criterion.

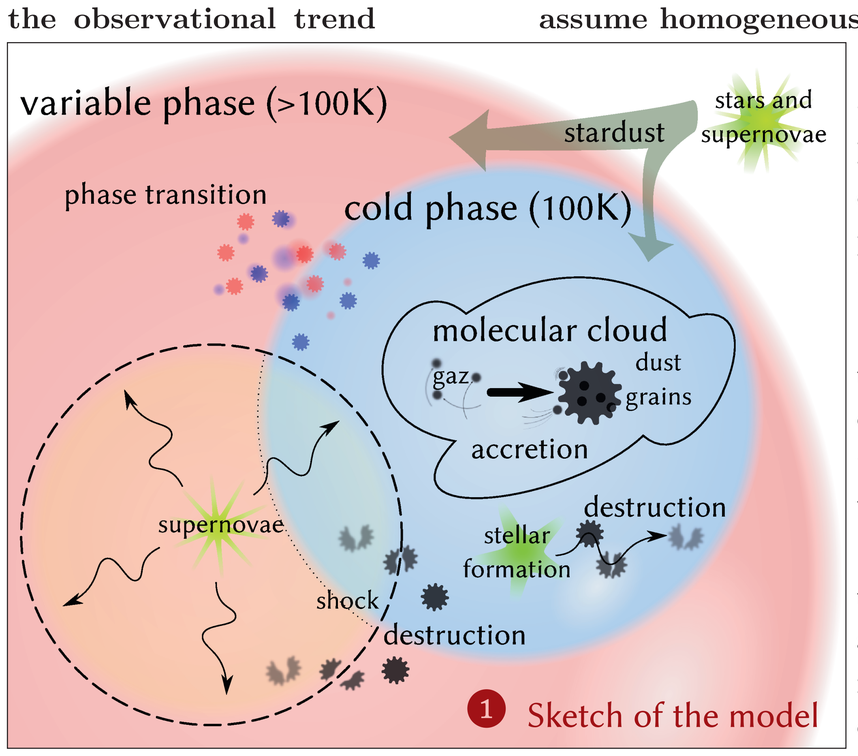

1 Sketch of the model

Model

During the simulation, the dust is produced and destroyed according to three main physical processes: accretion in ISM, release by AGB and SN (stardust), destruction by SN shocks.

Dust mass is computed separately in each phase of the SPH code and is transfered with condensation and evaporation of the CP. Transfers assume homogeneous dust abundances in each phase.

Stardust. The model includes the production from AGB and SN [1,11]. We use data from Zhukovska et al. [16] to compute a metallicity dependant production by stellar populations. Each phase receives a dust mass proportionnal to its volume.

Accretion [3]. It occurs only in CP and above a threshold of $n_{\rm H} = 10^4$ cm^{-3}. The accretion rate is estimated from the grain-gas collision rate [16], using the total of C, O, Mg, Si, Fe abundances, which are individually computed by our code.

Destruction. SN shocks are the main destructive mechanism [6]. From the gas mass shocked by a SN [5] and a destruction efficiency [6] we can derive the destroyed dust mass, proportionnal to the energy released during the SN feedback.

Results

We have performed four simulations to check the three physical processes: stardust (S), accretion (A) and destruction (D). Simulations are labelled according to the active processes. The model DSA implements the full physics.

We plot the mass fraction of oxygen (O) vs the dust one, for both observations [2,4,9,14] and our runs. For the observations each point is a galaxy. For our models we plot the values directly extracted from gas particles properties at some time of the simulations, as well as a density-weighted histogram using the SPH kernel.

The observational dust and oxygen abundances have been homogenised using the calibration of Draine et al. [2] with the theoretical O calibration [8] of Moustakas et al. [12]. Then, we apply an additional offset because this calibration overestimates abundance by 0.6 dex [7,12].

Snapshots at $t = 5.24$ Gyr

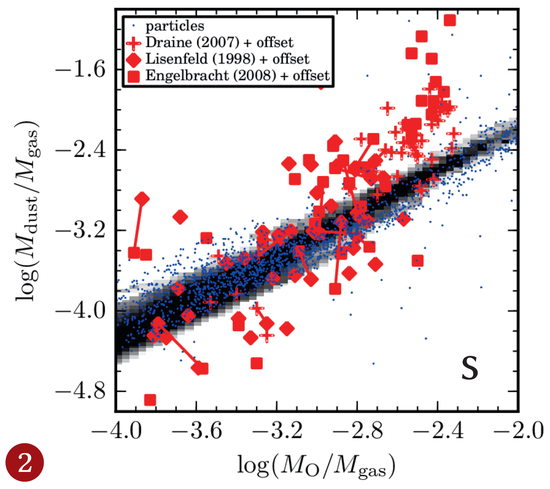

2

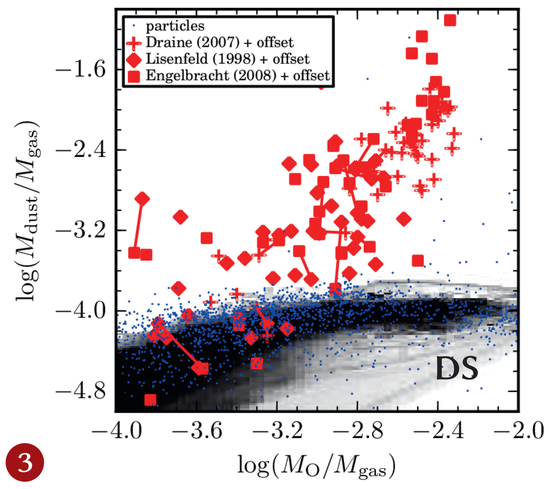

3

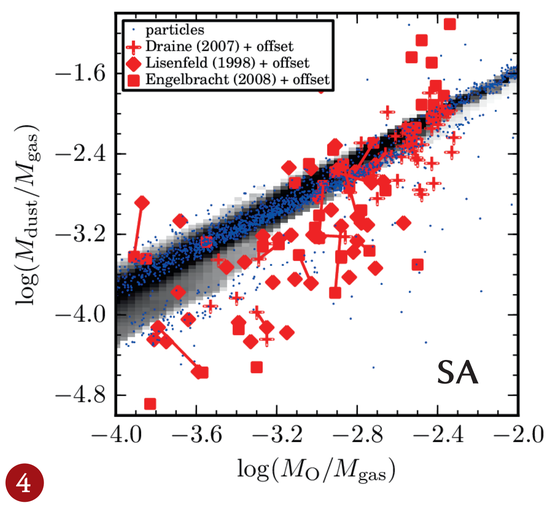

4

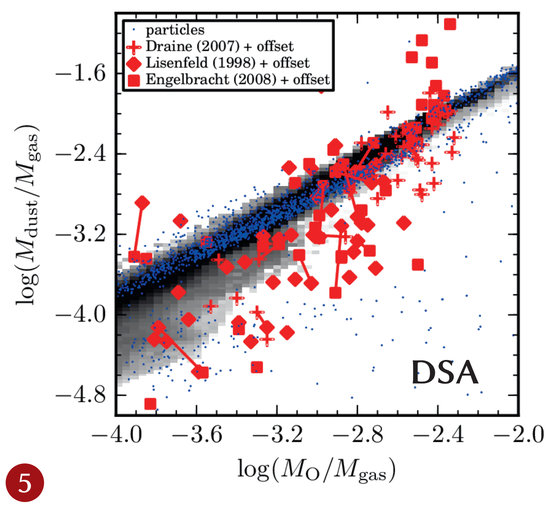

5

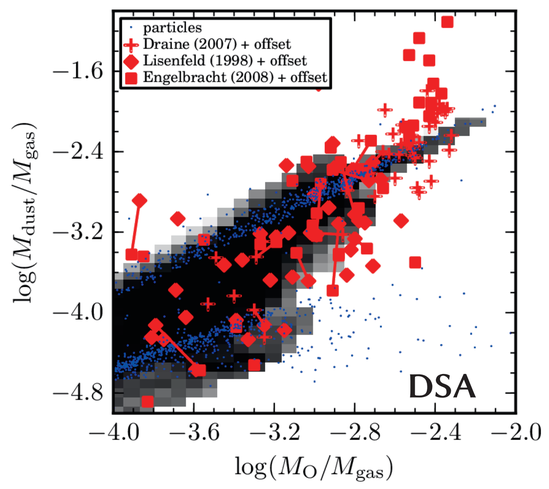

6 $t = 263$ Myr, SFR ~ 1 $M_\odot$/yr

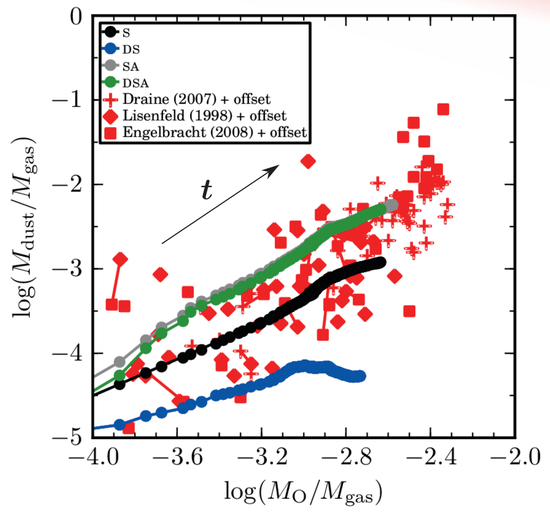

7 Snapshots, every ~ 25 Myr, in radius < 5 kpc

The agreement with the observed values is quite good but we can draw a few other conclusions from snapshots at $t = 5.24$ Gyr:

- Fig. 2 shows that stardust alone cannot explain the slope. The simulation overestimates the dust fraction, especially for low metallicity galaxies.
- In Fig. 3 the destruction can explain the low dust fraction of low metallicity dwarf galaxies.
- For Fig. 4 the high metallicity galaxies are better fitted with the accretion switched on.
- The full model DSA of the Fig. 5 is unable to reproduce the slope for the full range of metallicities.

If we select another time ($t = 263$ Myr), just after the SFR maximum, the DSA simulation provides better correlation with observations (see Fig. 6). Indeed, at that time, the higher SNII rate obviously destroys more dust. It must be noted that the destruction process does not have any free parameters, since the destruction efficiency comes from theoretical model of Jones et al. [6].

Fig. 7 shows the time evolution of the values computed every 25 Myr for a cylindrical radius < 5 kpc. Observed low-metallicity galaxies have high vertical dispersion and a non-linear slope. Few galaxies fall to the dust fraction of SD. This suggests that these galaxies are dominated by the dust destruction. Besides, comparison of Fig. 5 and Fig. 6 suggests that the effect of dust destruction is related to the star formation history.

Bibliography

[1] Cherchneff, I. & Dwek, E. 2010, ApJ, 713, 1

[2] Draine, B. T., Dale, D.A., Bendo, G., et al. 2007, ApJ, 663, 866

[3] Draine, B. T. 2009, ASPCS, vol. 414, 453–+

[4] Engelbracht, C. W., Rieke, G. H., Gordon, K. D., et al 2008, ApJ, 678, 804

[5] Hirashita, H., Tajiri, Y. Y., & Kamaya, H. 2002, A&A, 388, 439

[6] Jones, A. P., Tielens, A. G. G. M., & Hollenbach, D.J. 1996, ApJ, 469, 740

[7] Kewley, L. J., Ellison, S. L. 2008, ApJ, 681, 1183

[8] Kobulnicky, H. A. & Kewley, L. J. 2004, ApJ, 617, 240

[9] Lisenfeld, U. & Ferrara, A. 1998, ApJ, 496, 145

[10] Michel-Dansac, L. & Wozniak, H. 2004, A&A, 421, 863

[11] Morgan, H. L. & Edmunds, M. G. 2003, MNRAS, 343, 427

[12] Moustakas, J., Kennicutt, Jr., R. C., Tremonti, C.A., et al. 2010, ApJS, 190, 233

[13] Savage, B. D. & Sembach, K.R. 1996, ARA&A, 34, 279

[14] Walter, F., Cannon, J. M., Roussel, H., et al. 2007, ApJ, 661, 102

[15] Wozniak, H., Champavert, N., Feldner, H. 2010, EASPS, 44, 41

[16] Zhukovska, S., Gail, H., & Trieloff, M. 2008, A&A, 479, 453